J Vet Sci. 2023 Sep;24(5):e73
https://doi.org/10.4142/jvs.23141
pISSN 1229-845X·eISSN 1976-555X

Journal of Veterinary Science

Original Article

Molecular and Cellular Biology

Check for updates

Analysis of miRNA expression in the trachea of Ri chicken infected with the highly pathogenic avian influenza H5N1 virus

Suyeon Kang [1], **Thi Hao Vu** [1], **Jubi Heo** [1], **Chaeeun Kim** [1], **Hyun S. Lillehoj** [2], **Yeong Ho Hong** [1,*]

[1]Department of Animal Science and Technology, Chung-Ang University, Anseong 17546, Korea
[2]Animal Biosciences and Biotechnology Laboratory, Agricultural Research Services, United States Department of Agriculture, Beltsville, MD 20705, USA

OPEN ACCESS

Received: May 27, 2023
Revised: Jul 13, 2023
Accepted: Aug 17, 2023
Published online: Sep 6, 2023

***Corresponding author:**
Yeong Ho Hong
Department of Animal Science and Technology, Chung-Ang University, 4726 Seodong-daero, Daedeok-myeon, Anseong 17546, Korea.
Email: yhong@cau.ac.kr
https://orcid.org/0000-0002-4510-7851

ABSTRACT

Background: Highly pathogenic avian influenza virus (HPAIV) is considered a global threat to both human health and the poultry industry. MicroRNAs (miRNA) can modulate the immune system by affecting gene expression patterns in HPAIV-infected chickens.
Objectives: To gain further insights into the role of miRNAs in immune responses against H5N1 infection, as well as the development of strategies for breeding disease-resistant chickens, we characterized miRNA expression patterns in tracheal tissues from H5N1-infected Ri chickens.
Methods: miRNAs expression was analyzed from two H5N1-infected Ri chicken lines using small RNA sequencing. The target genes of differentially expressed (DE) miRNAs were predicted using miRDB. Gene Ontology and Kyoto Encyclopedia of Genes and Genomes analysis were then conducted. Furthermore, using quantitative real-time polymerase chain reaction, we validated the expression levels of DE miRNAs (miR-22-3p, miR-146b-3p, miR-27b-3p, miR-128-3p, miR-2188-5p, miR-451, miR-205a, miR-203a, miR-21-3p, and miR-200a-3p) from all comparisons and their immune-related target genes.
Results: A total of 53 miRNAs were significantly expressed in the infection samples of the resistant compared to the susceptible line. Network analyses between the DE miRNAs and target genes revealed that DE miRNAs may regulate the expression of target genes involved in the transforming growth factor-beta, mitogen-activated protein kinase, and Toll-like receptor signaling pathways, all of which are related to influenza A virus progression.
Conclusions: Collectively, our results provided novel insights into the miRNA expression patterns of tracheal tissues from H5N1-infected Ri chickens. More importantly, our findings offer insights into the relationship between miRNA and immune-related target genes and the role of miRNA in HPAIV infections in chickens.

Keywords: Influenza A virus; immunity; network analysis; signal transduction; high-throughput rna sequencing

ORCID iDs

Suyeon Kang
https://orcid.org/0000-0002-9435-9318
Thi Hao Vu
https://orcid.org/0000-0001-9098-6990
Jubi Heo
https://orcid.org/0000-0002-9869-3831
Chaeeun Kim
https://orcid.org/0009-0002-9482-5398
Hyun S. Lillehoj
https://orcid.org/0000-0001-7755-6216
Yeong Ho Hong
https://orcid.org/0000-0002-4510-7851

Author Contributions

Conceptualization: Kang S, Lillehoj HS, Hong YH; Data curation: Kang S, Hong YH; Formal analysis: Kang S; Funding acquisition: Hong YH; Investigation: Kang S, Heo J, Vu TH, Kim C, Lillehoj HS, Hong YH; Methodology: Kang S, Heo J, Vu TH, Kim C, Hong YH; Project administration: Hong YH; Resources: Hong YH; Software: Hong YH; Supervision: Hong YH; Validation: Kang S, Hong YH; Visualization: Kang S, Hong YH; Writing - original draft: Kang S; Writing - review & editing: Kang S, Lillehoj HS, Hong YH.

Conflict of Interest

The authors declare no conflicts of interest.

Funding

This research was funded by the National Research Foundation grant (NRF-2021R1A2C2005236) of the Republic of Korea.

INTRODUCTION

Avian influenza viruses (AIVs) are type A influenza viruses belonging to the family *Orthomyxoviridae* [1]. AIV is classified as a highly pathogenic avian influenza virus (HPAIV) and a low pathogenic avian influenza virus (LPAIV) based on pathogenicity tests and systemic versus local replication [2]. H5N1, a subtype of HPAIV, is considered a global threat to the poultry industry and human health [3]. LPAIV induces mild symptoms, such as a reduction in egg production, whereas HPAIV causes high mortality rates in chickens, resulting in substantial economic losses [4]. The incidence of cases of human infection by HPAIV, H5N1, has been steadily increasing over the past 20 years and the World Health Organization (WHO) reported that 455 out of 861 people infected with this virus died in 2019 [5].

MicroRNAs (miRNAs) are a small non-coding RNAs with a length of approximately 22 nucleotides [6]. miRNAs can post-transcriptionally regulate gene expression via mRNA degradation and translational repression [7]. By modulating the expression of genes related with the immune response, miRNAs may play regulatory roles in the immune system [8]. Moreover, specific miRNAs can control various immune-related pathways such as the Toll-like receptor (TLR) signaling pathway, mitogen-activated protein kinase (MAPK) signaling pathway, and PI3K-Akt signaling pathway [9]. Therefore, characterizing the mechanisms through which AIV impacts the expression of miRNAs that may control the immune response in chickens is crucial.

Several studies have performed small RNA sequencing (RNA-seq) in lung and immune organs such as the thymus, bursa of Fabricius, and spleen of H5N1-infected chickens [10-12]. Moreover, we previously conducted RNA-seq analyses of lung and trachea tissues of H5N1-infected Ri chicken [13,14]. In this study, we analyzed the expression of miRNAs and their target genes in tracheae from two genetically distinct Ri chicken lines infected with HPAIV H5N1, after which bioinformatic analyses were conducted to identify differentially expressed (DE) miRNAs and their target genes.

MATERIALS AND METHODS

Animals and infection

Animal experiments were conducted with a total of forty 4-week-old specific-pathogen-free Ri chickens, out of which 20 chickens were from an HPAIV-resistant line (*MX* genotype) and the remaining 20 chickens were from a susceptible line (*BF2* genotype) (**Supplementary Table 1**). Chickens with allele A at position 631 of *Mx* were selected for the resistant line, whereas those with allele G at the same position were selected for the susceptible line (**Supplementary Fig. 1**). Furthermore, based on the *BF2* genotyping, chickens exhibiting the *B21* haplotype were classified as resistant, whereas the chickens with the *B13* haplotype were classified as susceptible [14]. Therefore, *Mx*(A)/*B21* chickens were classified as resistant and *Mx*(G)/*B13* chickens were classified as susceptible.

A total of 20 Ri chickens from each line were intranasally inoculated with 200 μL of the harvested allantoic fluid of infected eggs that contained 1×10^4 titers of the A/duck/Vietnam/QB1207/2012, which was determined to be the egg infectious dose 50 for H5N1 [15]. The HPAIV challenge experiments were performed at the Department of Biochemistry and Immunology of the National Institute of Veterinary Research (NIVR), Vietnam, according to the Office International des Epizooties guidelines.

Trachea collection and total RNA extraction

Trachea samples were collected from euthanized chickens at 1 day post-infection (dpi) and 3 dpi, as recommended by the WHO manual on animal influenza diagnosis and surveillance. All animal protocols were approved by the NIVR, Vietnam (TCVN 8402:2010/TCVN 8400–26:2014).

All trachea samples were homogenized via cryogenic grinding and total RNA was extracted using the TRIzol reagent (Invitrogen, USA) according to the manufacturer's instructions.

Small RNA-seq and sequencing data analysis

The tracheal RNA quality was assessed using a Bioanalyzer RNA chip (Agilent Technologies, USA) and a Trinean DropSense96 micro-sample UV/VIS spectrophotometer (Trinean, Gentbrugge, Belgium). The samples that did not meet the QC and RIN value quality criteria (28S:18S > 1 and RIN > 7) were excluded from sequencing. A library was constructed using the TruSeq Small RNA Library Prep Set (Illumina, USA). Small RNA-seq was performed by LAS (Korea) using an Illumina NextSeq 500 system.

After sequencing, the raw reads were filtered using FastQC v0.11.5 (http://www.bioinformatics.babraham.ac.uk/projects/fastqc/). Skewer v0.2.2 (https://github.com/relipmoc/skewer/) was used for trimming the raw quality bases and sequencing adaptors. The processed reads were mapped to the reference genome (gg6) using QuickMIRSeq (https://sourceforge.net/projects/quickmirseq/files/). All known mature miRNA sequences were obtained from the miRbase database [16]. The expression level of miRNAs was calculated as reads per million reads. DE miRNAs were identified via statistical analysis using edgeR (Empirical Analysis of Digital Gene Expression Data in R).

Next, the target genes of the DE miRNAs were predicted using the miRDB MicroRNA Target Prediction Database (https://mirdb.org/) [17,18]. As recommended by the curators of the miRDB database, the target genes with target scores > 80 were used for Gene Ontology (GO) enrichment analysis and Kyoto Encyclopedia of Genes and Genomes (KEGG) enrichment analysis using GO resource (http://geneontology.org/) and David 2021 (https://david.ncifcrf.gov/) [19]. The results of our GO and KEGG pathway analyses were visualized using R [20]. The network between DE miRNAs and target genes related to immune response pathways was visualized using Cytoscape 3.9.0 [21].

Primer design

To validate the sequencing results, the known mature miRNA sequences obtained from miRBase v22.1 [16] were used for the forward primer, whereas the mRQ 3'-primer of the Mir-X miRNA qRT-PCR TB Green kit (TaKaRa Bio, Japan) was used as the reverse primer. Next, gene-specific primers were designed using Primer-BLAST (https://www.ncbi.nlm.nih.gov/tools/primer-blast/) to validate the expression level of the target genes of DE miRNAs. All primers were synthesized by Genotech (Korea) (**Table 1**).

Validation of expression of miRNA and target genes by quantitative real-time polymerase chain reaction (qRT-PCR)

cDNA for miRNA expression analysis was synthesized using the Mir-X miRNA First-Strand Synthesis kit (TaKaRa Bio) according to the manufacturer's instructions. The expression values of the miRNAs were determined using the Mir-X miRNA qRT-PCR TB Green kit (TaKaRa Bio) using a CFX Connect Real-Time PCR Detection System (Bio-Rad, USA) according to the manufacturer's recommendations. U1A was used as a reference gene for the assessment of relative differential expression.

Table 1. Primers used for quantitative real-time polymerase chain reaction

Genes	Sequences (5′→3′)
gga-miR-22-3p	AAGCTGCCAGTTGAAGAACTGT
gga-miR-27b-3p	TTCACAGTGGCTAAGTTCTGC
gga-miR-128-3p	TCACAGTGAACCGGTCTCTTT
gga-miR-146b-3p	CCCTATGGATTCAGTTCTGC
gga-miR-205a	TCCTTCATTCCACCGGAGTCTG
gga-miR-203a	GTGAAATGTTTAGGACCACTTG
gga-miR-2188-5p	AAGGTCCAACCTCACATGTCCT
gga-miR-451	AAACCGTTACCATTACTGAGTTT
gga-miR-200a-3p	TAACACTGTCTGGTAACGATGT
gga-miR-21-3p	CAACAACAGTCGGTAGGCTGTC
U1A	CTGCATAATTTGTGGTAGTGG
MAPK20	F: GGAAGCTCCAGTCAAAGTAA R: ATCCATGGAAAAGTACCCAC
MEF2C	F: CCCATTGGACTCACCAGACC R: TGCTATCATGTCGCCCATCC
PIK3R1	F: AGCAGGCGTAGATTAGAAGAG R: CTGAGTCAGCCACATCAAGTA
PLK2	F: TGCAGTAGAAGGTCAATGGC R: TCACCCAGTTTCAGTTCCAT
TRAF3	F: CGTCTCGGCGCCACTTAGGA R: GGGCAGCCAGACGCAATGTTCA
NFATC3	F: AACGAACGGTCTGGTCTTCC R: TTGGTGGTAGAGCTTGGCAG

To quantify the expression level of target genes, cDNA was synthesized using the Revert Aid First Strand cDNA Synthesis kit (Thermo Fisher Scientific, USA) according to the manufacturer's instructions. Briefly, 2 μg of total RNA was combined with 2 μL of DNase I, 1 μL of reaction buffer (10×), and nuclease-free water up to 10 μL. The mixture was then incubated at 37°C for 30 min. Afterward, the mixture was mixed with 1 μL of EDTA and incubated at 65°C for 10 min. Next, 4 μL of reaction buffer (5×), 1 μL of OligodT, 2 μL of dNTP (10 mM), 1 μL of RiboLock RNase Inhibitor (20 U/μL), and 1 μL of RevertAid M-MuLV RT (200 U/μL) were added to the mixture. The reaction mix was incubated at 42°C for 60 min and 72°C for 5 min. Then, 130 μL of nuclease-free water was added to the reverse-transcription reaction mixtures for dilution. Target gene expression level was determined using Dyne qPCR 2X PreMIX (Dyne Bio, Korea) in a CFX Connect Real-Time PCR Detection System (Bio-Rad) following the manufacturer's instructions. GAPDH was used as a reference gene. All qRT-PCR assays were conducted in triplicate. miRNA and target gene differential expression were calculated using the $2^{-\Delta\Delta Ct}$ method [22].

Statistical analysis

Statistical analyses were performed using the SPSS software (version 25.0; IBM, USA). All data were expressed as the mean ± standard error of the mean. Student's *t*-test was conducted to identify unpaired differences in expression between the experimental groups. The $p < 0.05$ was considered statistically significant.

RESULTS

Analysis of small RNA-seq

Small RNA-seq was performed to determine the miRNA expression in the control and H5N1-infected Ri chickens. A total of 24 trachea RNA samples at 1 dpi and 3 dpi that passed the quality criteria were used for small RNA-seq analysis. The infected chickens exhibited most of the typical

https://doi.org/10.4142/jvs.23141

Table 2. Distribution of small RNA sequences from trachea samples of the control and H5N1-infected Ri chickens

Variables	miRNA (%)	Hairpin (%)	Small RNA (%)	mRNA (%)	Unaligned (%)
S2D3-CTR	64.89	0.11	2.15	2.67	30.19
S1D3-HPAI	71.43	0.12	2.49	0.88	25.08
S2D3-HPAI	75.88	0.16	2.52	0.79	20.65
S3D3-HPAI	72.96	0.15	2.86	1.05	22.98
S5D3-HPAI	71.10	0.14	3.18	0.91	24.67
R1D3-CTR	73.15	0.15	2.70	0.93	23.07
R2D3-CTR	59.55	0.20	6.72	2.37	31.16
R1D3-HPAI	67.05	0.17	3.77	1.83	27.19
R2D3-HPAI	36.33	0.17	5.54	3.57	54.38
R3D3-HPAI	61.54	0.17	4.11	1.23	32.95
R5D3-HPAI	71.70	0.16	4.41	0.77	22.96

Unaligned reads were defined as reads that were not aligned to the reference genome.

symptoms of HPAIV at 3 dpi and 11 of these 3 dpi samples were used for analyzing the small RNA-seq. The results of the read quality check are summarized in **Supplementary Table 2**. In the susceptible line, 39.1 million raw read pairs were obtained in the control group and 41.3–46.5 million read pairs were obtained in the infected group (**Supplementary Table 2**). A total of 35.5 million clean read pairs were obtained for the control, whereas 37.0–43.6 million clean read pairs were obtained for the infection group at 3 dpi (**Supplementary Table 2**). The ratio of the raw and clean read base pairs with a Phred quality score of ≥ 30 (Q30) exceeded 80% for all of the examined sequences (**Supplementary Table 2**). A total of 36.1–36.6 million raw read pairs were obtained before processing. After processing, the clean read pairs ranged from 31.7 to 37.1 million in the resistant line (**Supplementary Table 2**).

The ratio of miRNAs accounted for an average of 66% in the control and 59% in the resistant line (**Table 2**). The ratio of miRNAs accounted for 65% in the control and 73% in the susceptible line (**Table 2**).

Next, the clean reads were aligned to the reference genome (gg6). A total of 472 mature miRNAs were mapped to the reference genome in both the susceptible and resistant lines. In the susceptible line, 152 miRNAs were identified as DE in the infection group, with DE sequences being defined as those with a $|\log_2\text{fold change}| \geq 1$ and $p < 0.05$ (**Fig. 1A**, **Supplementary Table 3**). A total of 81 miRNAs were downregulated and 71 miRNAs were upregulated in the infection group compared with the control group (**Fig. 1A**, **Supplementary Table 3**). Particularly, gga-miR-6640-5p exhibited the lowest $\log_2$ fold change (−5.88-fold), whereas gga-miR-1684b-3p exhibited the highest $\log_2$ fold change (−10.15-fold) (**Supplementary Table 3**). A total of 46 DE miRNAs were identified in the resistant line, among which 21 miRNAs were downregulated and 25 miRNAs were upregulated in the infection samples compared with the control (**Fig. 1B**, **Supplementary Table 3**). From these samples, gga-miR-1755 exhibited the lowest $\log_2$ fold change (−2.79-fold), whereas gga-miR-1682 showed the highest $\log_2$ fold change (5.42-fold) (**Supplementary Table 3**). A total of 53 DE miRNAs were identified in the infection group of the resistant line compared to the infection group of the susceptible line (**Fig. 1C**, **Supplementary Table 3**). In this comparison, gga-miR-1684b-3p exhibited the lowest $\log_2$ fold change (−2.62-fold), whereas gga-miR-7b showed the highest $\log_2$ fold change (9.53-fold) (**Supplementary Table 3**).

In previous study, gene expression patterns on trachea from H5N1-infected Ri chicken were analyzed by RNA-seq [13]. Few DE miRNAs in infection samples of resistant line and susceptible line were showed negative correlation with DE genes from RNA-seq result

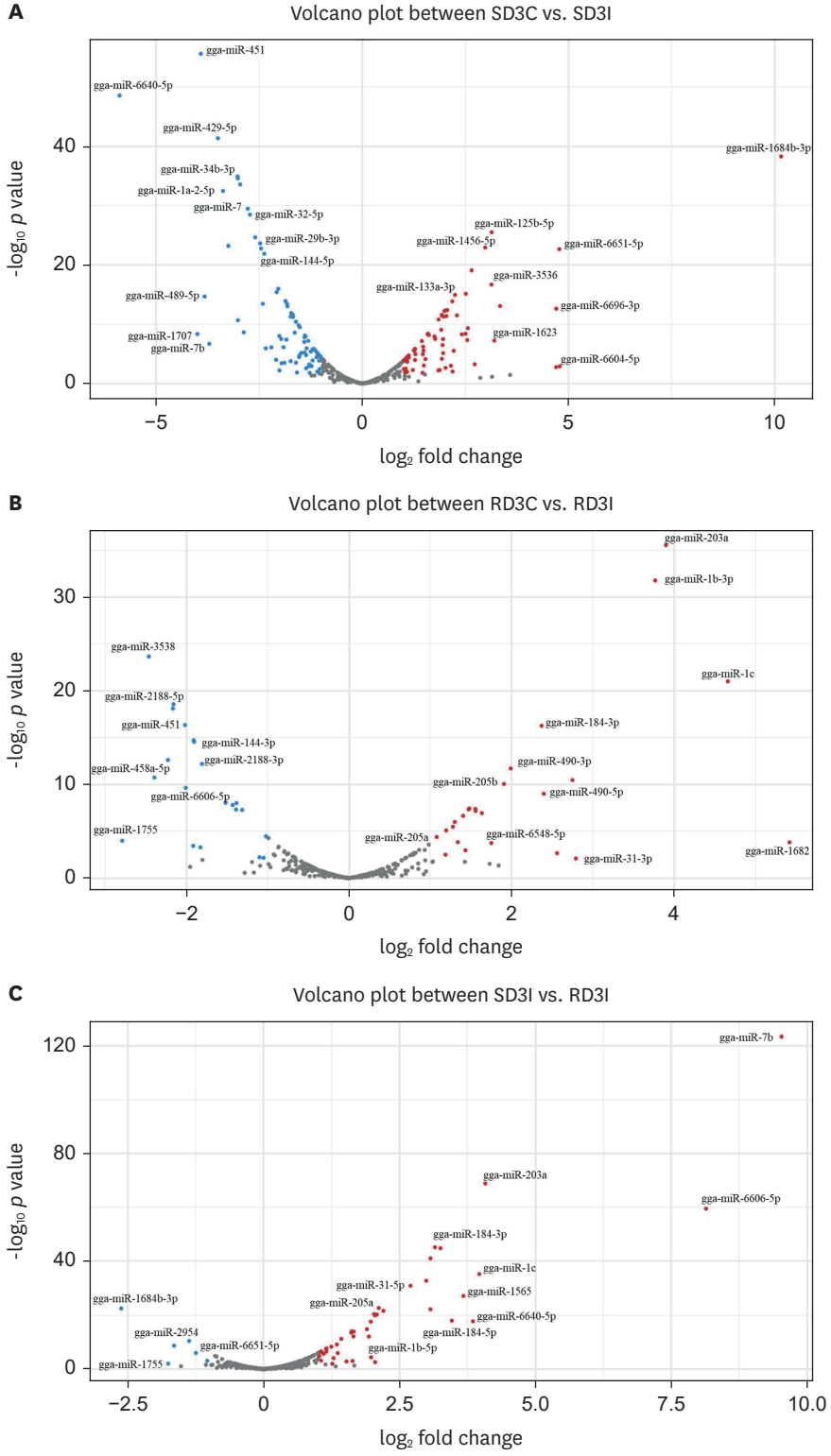

Fig. 1. Volcano plot and hierarchical clustering analysis of differentially expressed miRNAs in Ri chickens. (A-C) Volcano plot: (A) susceptible line, (B) resistant line, (C) comparison between the infection groups of the resistant and susceptible Ri chicken lines. X-axis: $\log_2$ fold change; Y-axis: $-\log_{10}$ *p* value. The blue dots indicate downregulated DE miRNAs and the red dots indicate upregulated DE miRNAs with $|\log_2\text{fold change}| \geq 1$ and $p < 0.05$.
DE, differentially expressed; miRNA, microRNA.

https://doi.org/10.4142/jvs.23141

that conducted with same tracheal RNA samples (**Supplementary Table 4**). A total of 5 DE miRNAs were down-regulated and 10 target genes were up-regulated in infection group of the resistant line compared with the susceptible line (**Supplementary Table 4**). A total of 38 up-regulated DE miRNAs demonstrated negative correlation with 139 target genes that up-regulated in infection samples of the resistant line against the susceptible line (**Supplementary Table 4**).

Target genes prediction and bioinformatic analysis

Next, miRDB (https://mirdb.org/) was used to predict the target genes of the 53 miRNAs that were identified as DE in the resistant line compared with the susceptible line in the infection samples. A total of 3,755 target genes with scores higher than 80 were predicted from 53 DE miRNAs (**Supplementary Table 5**). Bioinformatic analyses were performed using the 3,755 target genes and the top 30 terms with a false discovery rate (FDR) < 0.05 and fold enrichment > 1 were illustrated in **Fig. 2**. Particularly, the Biological Process GO category mainly included neuron development, cell morphogenesis, and neuron projection development (**Fig. 2A**). The molecular function (MF) terms were mainly associated with MF, binding, and ion binding (**Fig. 2B**). The cellular component category mainly included pathways associated with the nucleus, plasma membrane, and the endomembrane system (**Fig. 2C**). To understand the biological functions of the target genes, KEGG pathway analysis was conducted using the DAVID database (FDR< 0.05). According to the KEGG pathway analysis results, the target genes were mainly related to the MAPK signaling pathway, endocytosis, adherens junction, and SNARE interactions in vesicular transport (**Fig. 2D**).

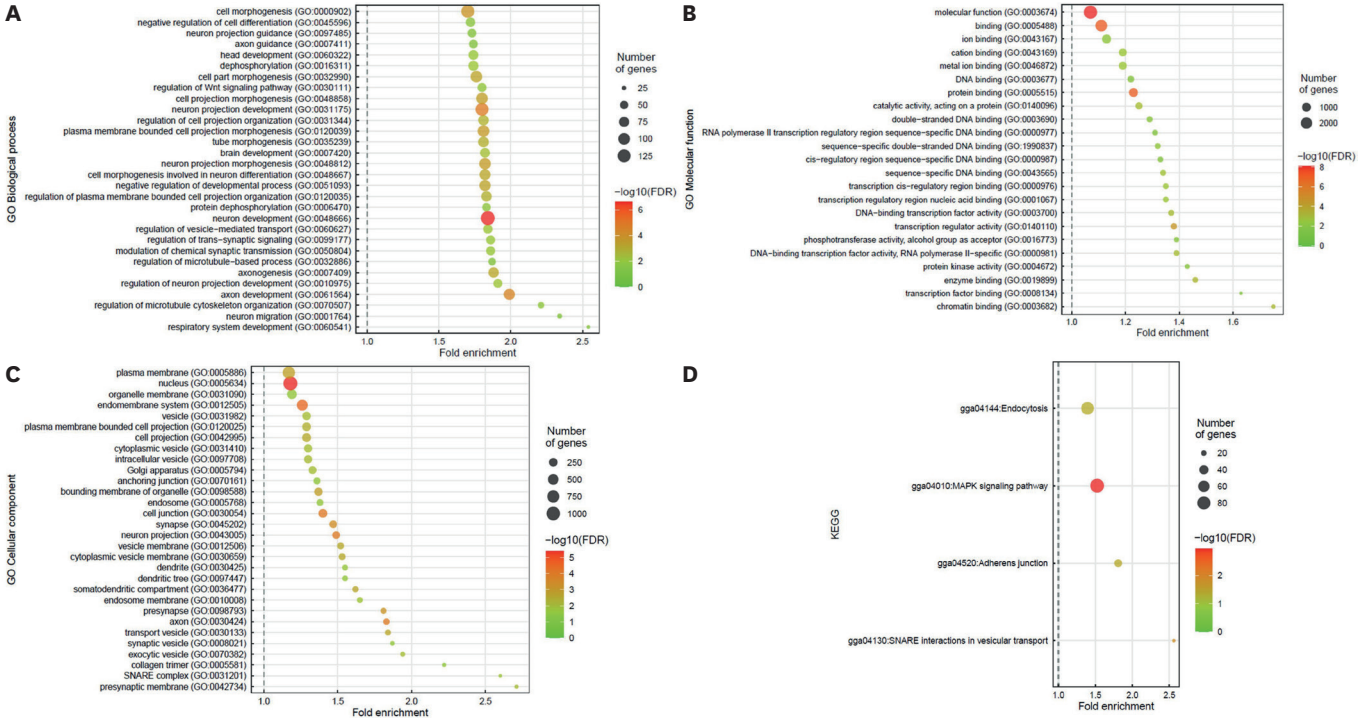

Fig. 2. Bioinformatic analysis of predicted target genes of differentially expressed microRNAs from infection group of resistant line compared with susceptible line. (A) Biological process, (B) molecular function, (C) cellular component, (D) KEGG pathway.
GO, Gene Ontology; KEGG, Kyoto Encyclopedia of Genes and Genomes; FDR, false discovery rate.

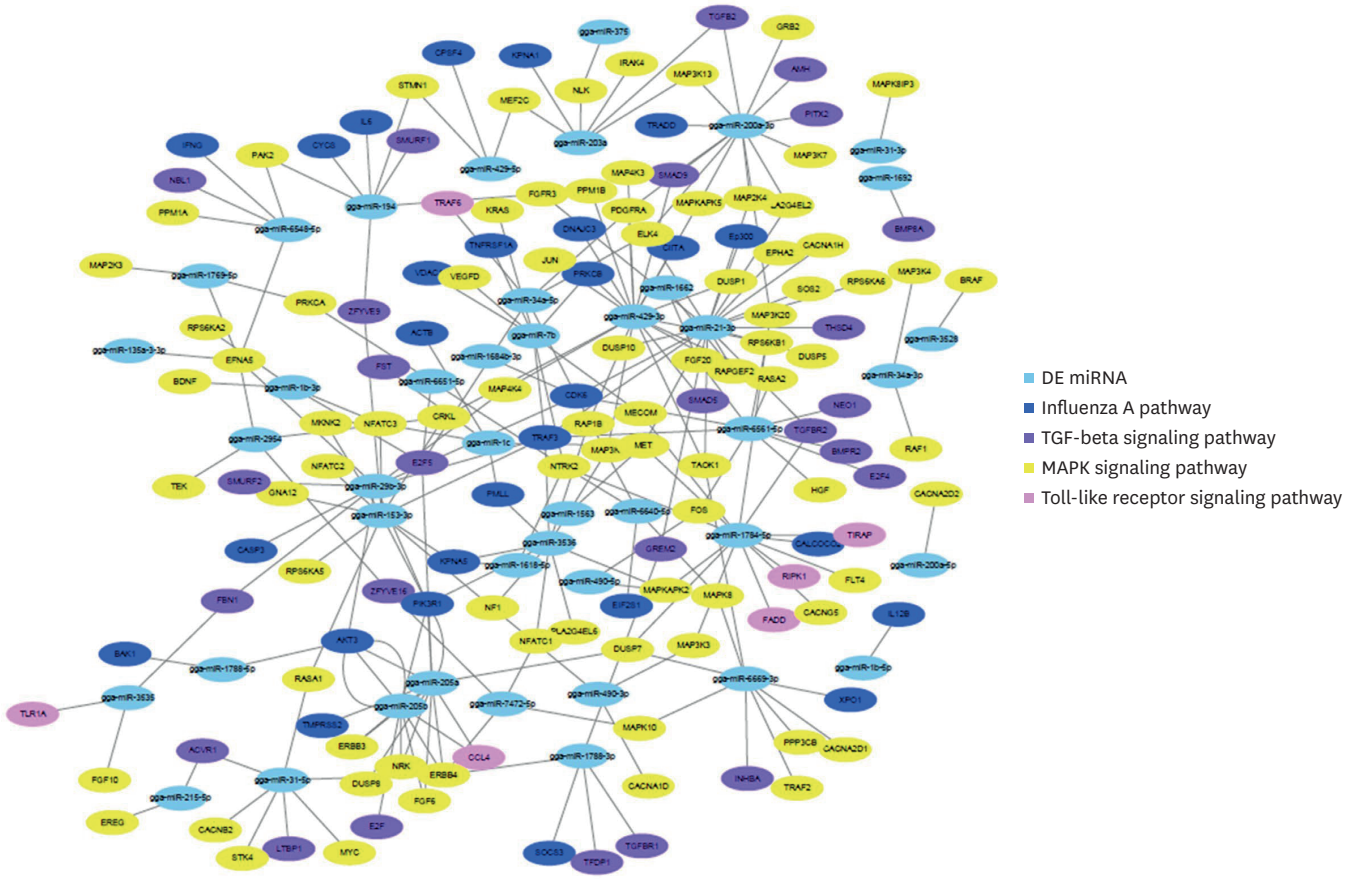

Fig. 3. Network interaction between DE miRNAs and target genes related to immune response pathways. DE miRNAs were identified by comparing the infection samples of the resistant line and those of the susceptible line. The colors indicate the main pathways involved in the immune system and/or avian influenza virus. DE, differentially expressed; miRNA, microRNA; TGF, transforming growth factor; MAPK, mitogen-activated protein kinase.

Additionally, we analyzed the interaction between 53 DE miRNAs and their target genes related to the immune response pathway and/or AIV by building a gene network using the Cytoscape software. A total of 238 interactions were identified between 53 DE miRNAs and 153 target genes, which were not overlapped (**Fig. 3**). The results of our network analysis suggested that these 53 DE miRNAs may target genes associated with the influenza A pathway, the transforming growth factor (TGF)-beta signaling pathway, the MAPK signaling pathway, and the TLR signaling pathway (**Fig. 3**).

Validation of DE miRNAs and predicted target gene expression

qRT-PCR was conducted to validate the results of the small RNA-seq of the 3 dpi samples. Specifically, we validated four miRNAs that were selected based on the read counts, their function in the immune system, and the number of target genes related to the immune response in each comparison (**Fig. 4**, **Supplementary Table 6**). Particularly, gga-miR-22-3p, gga-miR-146b-3p, gga-miR-27b-3p, and gga-miR-128-3p were upregulated in the infection samples compared with the control samples of the susceptible line (**Fig. 4**, **Supplementary Table 6**). In the resistant line, gga-miR-2188-5p, and gga-miR-451 were downregulated in the infection samples compared to the control (**Fig. 4**, **Supplementary Table 6**). In contrast, gga-miR-205a and gga-miR-203a were upregulated in the infected samples compared to the control (**Fig. 4**, **Supplementary Table 6**). Upon comparing the infection samples of the resistant and susceptible lines, gga-miR-21-3p, gga-miR-200a-3p, gga-miR-205a, and gga-

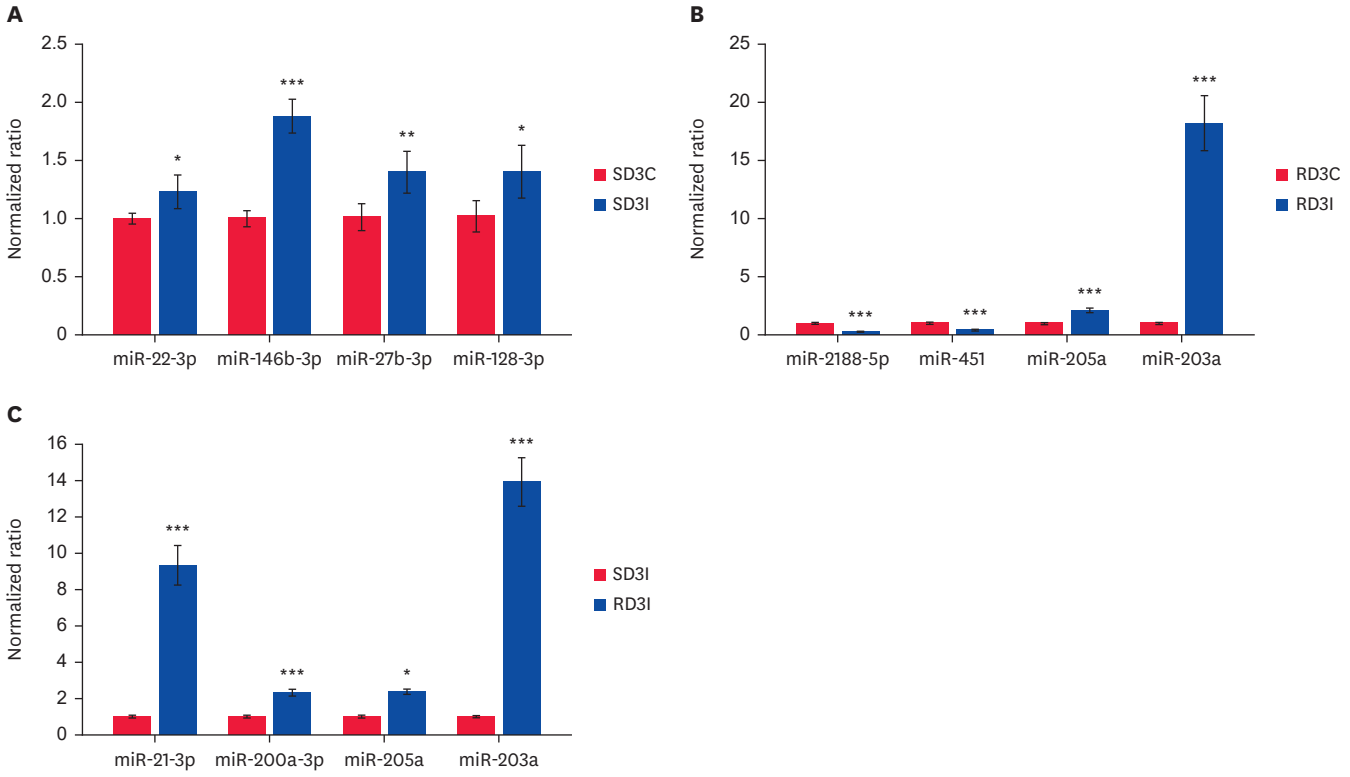

Fig. 4. Validation of DE miRNAs using qRT-PCR. (A) DE miRNAs in the infection group compared with the control group in the susceptible line. (B) DE miRNAs in the infection group compared with the control group in the resistant line. (C) DE miRNAs in the infection samples in the resistant line compared with the susceptible line. The expression level of miRNAs was normalized to the expression of the U1A gene. The error bars indicate the standard error of the mean. qRT-PCR was performed using pooled samples in triplicate. Some RNA samples did not pass the quality control criteria. In these cases, other samples from different batches were used for the validation of sequencing results (SD3C: S2D3C, S3D3C, S5D3C; SD3I: S1D3I, S2D3I, S3D3I, S5D3I; RD3C: R1D3C, R2D3C, R4D3C; RD3I: R1D3I, R2D3I, R3D3I, R5D3I).
DE, differentially expressed; miRNA, microRNA; qRT-PCR, quantitative real-time polymerase chain reaction.
*$p < 0.05$; **$p < 0.01$; ***$p < 0.001$.

miR-203a were found to be upregulated in the resistant line (**Fig. 4**, **Supplementary Table 6**). More importantly, the results of our qRT-PCR validation experiments were highly consistent with those of our small RNA-seq analyses (**Fig. 4**).

Furthermore, we also analyzed the expression levels of the target genes of the validated DE miRNAs. *TRAF3* was identified as the target gene of gga-miR-22-3p and its expression level was downregulated in the infection samples compared with the control samples in the susceptible line (**Supplementary Table 6**, **Fig. 5A**). The expression level of *NFATC3*, which was expected to be regulated by gga-miR-27b-3p, was also downregulated in the infection samples compared to the control samples in the susceptible line (**Supplementary Table 6**, **Fig. 5A**). *PI3KR1* was one of the target genes associated with gga-miR-205a and PLK2 was expected to be the target gene of gga-miR-2188-5p (**Supplementary Table 6**). In the resistant line, *PI3KR1* was downregulated and *PLK2* was upregulated in the infection samples compared to the control (**Fig. 5B**). Moreover, *MAP3K20* and *MEF2C* were downregulated in the infection group of the resistant line compared to the susceptible line (**Fig. 5C**). *MAP3K20* and *MEF2C* were predicted to be the target genes of gga-miR-200a-3p and gga-miR-203a, respectively.

https://doi.org/10.4142/jvs.23141

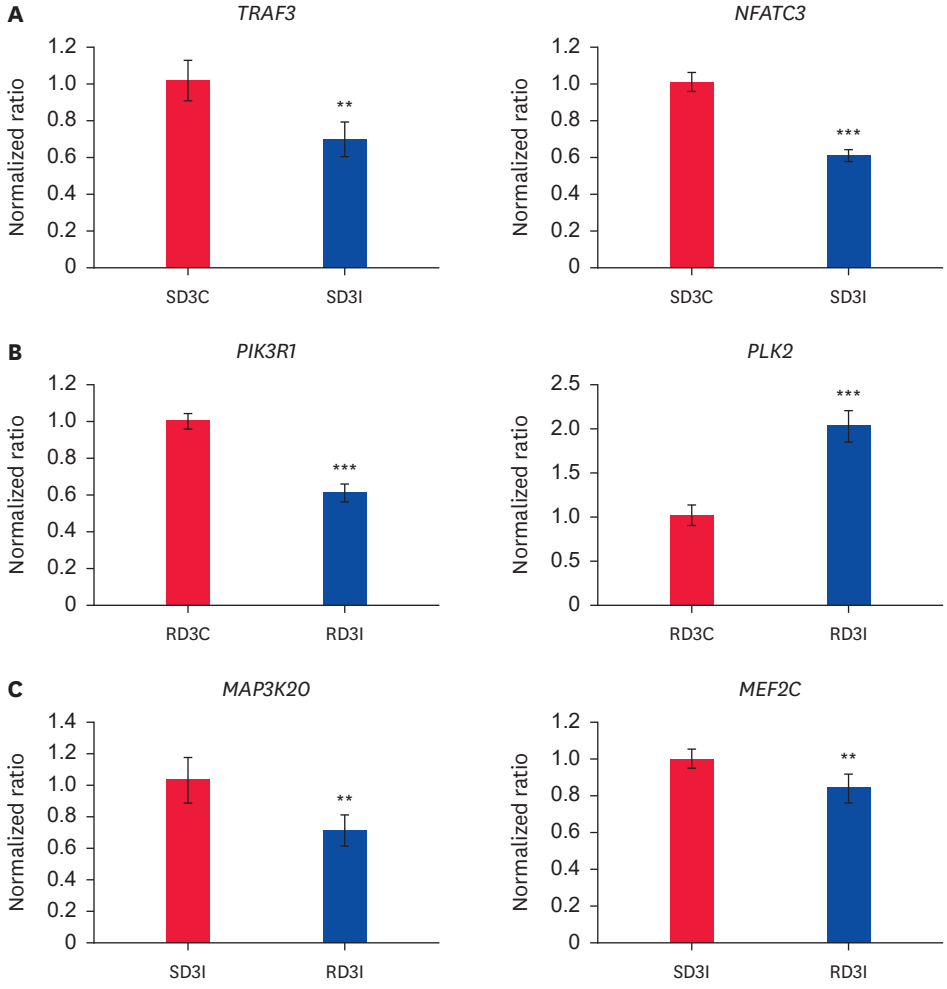

Fig. 5. qRT-PCR results of predicted target genes of differentially expressed microRNAs. (A) gga-miR-22-3p target expression of *TRAF3* and *gga-miR-27b-3p* target expression of *NFATC3* in susceptible control and infection samples at 3 dpi. (B) gga-miR-205a target expression of *PIK3R1* and gga-miR-2188-5p target expression of *PLK2* in resistant control and infection samples at 3 dpi. (C) gga-miR-200a-3p target expression of *MAP3K20* and gga-miR-203a target expression of *MEF2C* in infection samples of resistant line compared with the susceptible line at 3 dpi. The expression level of genes was normalized to the expression of *GAPDH*. The error bars represent the standard error of the mean. qRT-PCR was performed using pooled samples in triplicate.
qRT-PCR, quantitative real-time polymerase chain reaction; dpi, day post-infection.
$^{**}p < 0.01$; $^{***}p < 0.001$.

DISCUSSION

In this study, small RNA-seq analyses were conducted to characterize the expression of miRNAs in two distinct H5N1-infected Ri chicken lines (HPAIV-resistant and -susceptible) to identify the mechanisms through which AIV affects the expression of miRNAs associated with the modulation of the immune response during AIV infection. Ri chickens (i.e., the most commonly grown indigenous chickens in Vietnam farms) were classified as susceptible or resistant to AIV via genotyping of the *Mx* and *BF2* genes, respectively [23,24]. miRNA can regulate the innate and adaptive immune response by modulating the production/release of cytokines and chemokines and controlling the development/differentiation of adaptive immune cells such as B and T cells [9]. Due to the role of miRNA in immune regulation, miRNA expression patterns have been analyzed for various viruses that affect chickens over the past decade, including AIV and Newcastle disease virus [11,25]. To identify the mechanisms through which AIV influences the expression of miRNA and the role of miRNAs

https://doi.org/10.4142/jvs.23141

in host immune responses, small RNA-seq analyses were conducted to identify DE miRNAs in H5N1-infected chickens.

Our analysis of the interaction network between DE miRNAs and immune-related target genes revealed that DE miRNAs affect gene pathways involved in AIV infection such as the influenza A pathway, as well as the TGF-beta, MAPK, and TLR signaling pathways. These findings suggest that these DE miRNAs play an important role in the immune response against AIV. Several studies have demonstrated that the TGF-beta, MAPK, and TLR signaling pathways play a vital role in influenza A virus infection [26-28]. The exogenous TGF-beta delayed the mortality of H5N1-infected mice and depleted viral titers via the neutralization of TGF-beta during H5N1 infection [26]. Influenza A virus infection activates the Raf, MEK, ERK, and p38 genes, all of which are key components of the MAPK signaling pathway [27]. MAPK modulates the inflammatory responses and T-cell response against the influenza A virus [27]. TLR ligands play a critical role in the initiation and modulation of antiviral responses and can reduce the shedding of AIV in the trachea [28]. Our results demonstrated that the DE miRNAs between the infection samples of the resistant and susceptible lines may regulate the H5N1 virus infection by controlling the expression of target genes associated with the TGF-beta, MAPK, and TLR signaling pathways.

Furthermore, our findings indicated that gga-miR-146b-3p was upregulated in the infection samples compared to the control samples of the susceptible line. Specifically, gga-miR-146b-3p regulates autophagy and apoptosis by inhibiting the expression of AKT serine/threonine kinase 1 [29]. The AIV NS1 protein activates *PI3K* to prevent apoptosis for virus replication [30].

gga-miR-27b-3p was upregulated in the infection samples compared with the control samples in the susceptible line. gga-miR-27b-3p was also upregulated in infectious bursal disease virus-infected DF-1 cells, which inhibited the replication of infectious bursal disease virus and improved the expression of type I interferons such as IRF3 and IFN-β by targeting *SOCS3* and *SCOS6* expression [31].

In the resistant line, gga-miR-451 was downregulated in the infection samples compared with the control. gga-miR-451 was upregulated in lung tissues and DF-1 cells of *Mycoplasma gallisepticum*-infected chickens [32]. Moreover, gga-miR-451 could decrease the secretion of inflammatory cytokines and promote apoptosis to ensure efficient *M. gallisepticum* replication by repressing the expression of *YWHAZ* [32]. These results indicated that the downregulation of gga-miR-451 caused by AIV infection promoted inflammatory cytokine secretion and apoptosis in the resistant line.

Furthermore, gga-miR-200a-3p was upregulated in the infection samples of the resistant line compared to the susceptible line. gga-miR-200a-3p was also upregulated in the intestinal mucosal layer of chickens during necrotic enteritis infection [33]. In this study, gga-miR-200a-3p was found to suppress the expression of *TGFβ2*, *MAP2K4*, and *ZAK*, which are involved in the MAPK signaling pathway [33].

gga-miR-429-3p exhibited the highest number of interactions with target genes involved in influenza A virus-related pathways. gga-miR-429-3p can affect the TGF-beta pathway by regulating the expression level of *TGFβ1* [34].

This study also analyzed the expression levels of predicted target genes of DE miRNAs between infection samples from the susceptible and resistant lines. We predicted that gga-miR-22-3p and gga-miR-27b-3p may target *TRAF3* and *NFATC3*, respectively. Furthermore, gga-miR-22-3p and gga-miR-27b-3p were upregulated in the infection samples compared with the control samples of the susceptible line, which coincided with a downregulation of the *TRAF3* and *NFATC3* target genes. *TRAF3* may affect the replication of the influenza A virus and prevent its immune evasion by promoting the production of type I IFNs [35]. The NFAT family could regulate the production of immunomodulatory cytokines such as IL-2, IL-4, IFN-γ, and TNF-α in various immune cells [36].

gga-miR-205a was upregulated in the infection samples compared to the control samples in the resistant line and this coincided with a downregulation of *PIK3R1*, which was the predicted target gene. Depending on the viral strain, the influenza A virus can affect the PI3K signaling pathway, which is involved in viral entry. Particularly, the PI3K/AKT signaling pathway could facilitate the internalization of the influenza A virus [37].

gga-miR-2188-5p was downregulated in the infection samples of the resistant line and its target gene *PLK2* was upregulated. *PLK2* plays a critical role in the cell cycle, inflammation, and antiviral immunity [38].

Our findings also revealed that gga-miR-200a-3p and gga-miR-203a were upregulated in the infection samples of the resistant line compared with the susceptible line. However, their target genes, *MAP3K20* and *MEF2C*, were downregulated. Both the *MAP3K20* and *MEF2C* genes are involved in the MAPK signaling pathway. In a previous study, we demonstrated that gga-miR-200a-3p could repress ZAK, MAP2K4, and TGFβ2 expression using a luciferase assay [33]. *MP3K20* is a known activator of ERK, JNK, and p38, which are major MAPK pathways [39]. Moreover, *MEF2C* activity is directly related to the stimulation of B cell receptors, which are involved in the adaptive immune system, and its activation regulates B cell proliferation via the p38 MAPK cascade [40]. In this study, our findings demonstrated that the predicted target genes had a negative correlation with the identified DE miRNAs, and these genes were involved in various immune responses such as apoptosis, regulation of cytokine expression, viral replication, and proliferation of immune cells.

Several studies identified miRNA expression on H5N1 infection [11,12]. When comparing miRNA expression pattern with previous studies only few miRNAs showed similar pattern with our study. Gga-miR-7b was up-regulated in lung, spleen, thymus, and bursa of Fabricius from H5N1-infected chickens as up-regulated in RD3I samples compared with SD3I samples [11,12]. Few miRNAs such as gga-miR-216b, gga-miR-29b-3p, and miR-7 were also down-regulated in infection group compared with control group in lung [12], but were not significantly expressed in our experiment [10]. Furthermore, target genes of down-regulated miRNAs in lung were also enriched in MAPK signaling pathway as KEGG pathway analysis result in this study [12]. Taken together, miRNA expression pattern may depend on the time for virus infection and tissues.

In summary, the current study aimed to characterize the expression and potential role of miRNAs in the tracheal tissues of two distinct genetic lines (HPAIV-resistant and HPAIV-susceptible) of H5N1-infected Ri chickens by conducting small RNA-seq analysis. A total of 152 and 46 DE miRNAs were identified in the infection samples compared to the control samples in the susceptible and resistant lines, respectively. In the infection group, 53 DE

miRNAs were identified in the resistant chicken line compared to the susceptible chicken line. The results of our bioinformatic analyses revealed that most of the DE miRNAs in the infection samples of the susceptible line relative to the resistant line may modulate the MAPK signaling pathway. Moreover, network analyses between DE miRNAs and target genes elucidated interactions involved in various pathways related to AIV infection. Collectively, our findings provide novel insights into the role of miRNAs in the immune response against HPAIV H5N1 infection in chickens.

ACKNOWLEDGEMENTS

The authors thank the Department of Biochemistry and Immunology Laboratory of the National Institute of Veterinary Research, Vietnam, for conducting the animal experiments described in this study.

SUPPLEMENTARY MATERIALS

Supplementary Table 1
Number of Ri chickens used for avian influenza viruses challenge

Click here to view

Supplementary Table 2
Read quality check of the control and H5N1-infected trachea samples in Ri chickens

Click here to view

Supplementary Table 3
DE miRNAs in the H5N1-infected Ri chickens

Click here to view

Supplementary Table 4
Relationship between miRNA and mRNA sequencing of H5N1-infected trachea tissues at 3 day post-infection (resistant line vs. susceptible line)

Click here to view

Supplementary Table 5
List of all target genes of DE miRNAs from comparisons between infection samples in the resistant line compared with the susceptible line

Click here to view

Supplementary Table 6
List of validated differentially expressed miRNAs and immune-related target genes

Click here to view

Supplementary Fig. 1

Sequencing chromatogram of the Mx gene of Ri chickens.

Click here to view

REFERENCES

1. Lee CW, Saif YM. Avian influenza virus. Comp Immunol Microbiol Infect Dis. 2009;32(4):301-310.
PUBMED | CROSSREF
2. Suarez DL, Schultz-Cherry S. Immunology of avian influenza virus: a review. Dev Comp Immunol. 2000;24(2-3):269-283.
PUBMED | CROSSREF
3. Peiris JS, de Jong MD, Guan Y. Avian influenza virus (H5N1): a threat to human health. Clin Microbiol Rev. 2007;20(2):243-267.
PUBMED | CROSSREF
4. Neumann G, Chen H, Gao GF, Shu Y, Kawaoka Y. H5N1 influenza viruses: outbreaks and biological properties. Cell Res. 2010;20(1):51-61.
PUBMED | CROSSREF
5. Nuwarda RF, Alharbi AA, Kayser V. An overview of influenza viruses and vaccines. Vaccines (Basel). 2021;9(9):1032.
PUBMED | CROSSREF
6. Huang Y, Shen XJ, Zou Q, Wang SP, Tang SM, Zhang GZ. Biological functions of microRNAs: a review. J Physiol Biochem. 2011;67(1):129-139.
PUBMED | CROSSREF
7. Ha M, Kim VN. Regulation of microRNA biogenesis. Nat Rev Mol Cell Biol. 2014;15(8):509-524.
PUBMED | CROSSREF
8. Contreras J, Rao DS. MicroRNAs in inflammation and immune responses. Leukemia. 2012;26(3):404-413.
PUBMED | CROSSREF
9. Momen-Heravi F, Bala S. miRNA regulation of innate immunity. J Leukoc Biol. 2018;103(6):1205-1217.
PUBMED | CROSSREF
10. Lee S, Kang S, Heo J, Hong Y, Vu TH, Truong AD, et al. MicroRNA expression profiling in the lungs of genetically different Ri chicken lines against the highly pathogenic avian influenza H5N1 virus. J Anim Sci Technol. 2023;65(4):838-855.
CROSSREF
11. Li Z, Zhang J, Su J, Liu Y, Guo J, Zhang Y, et al. MicroRNAs in the immune organs of chickens and ducks indicate divergence of immunity against H5N1 avian influenza. FEBS Lett. 2015;589(4):419-425.
PUBMED | CROSSREF
12. Mishra A, Asaf M, Kumar A, Kulkarni DD, Sood R, Bhatia S, et al. Differential miRNA expression profiling of highly pathogenic avian influenza virus H5N1 infected chicken lungs reveals critical microRNAs, biological pathways and genes involved in the molecular pathogenesis. Virol Sin. 2022;37(3):465-468.
PUBMED | CROSSREF
13. Lee J, Hong Y, Vu TH, Lee S, Heo J, Truong AD, et al. Influenza A pathway analysis of highly pathogenic avian influenza virus (H5N1) infection in genetically disparate Ri chicken lines. Vet Immunol Immunopathol. 2022;246:110404.
PUBMED | CROSSREF
14. Vu TH, Heo J, Hong Y, Kang S, Tran HT, Dang HV, et al. HPAI-resistant Ri chickens exhibit elevated antiviral immune-related gene expression. J Vet Sci. 2023;24(1):e13.
PUBMED | CROSSREF
15. Huprikar J, Rabinowitz S. A simplified plaque assay for influenza viruses in Madin-Darby kidney (MDCK) cells. J Virol Methods. 1980;1(2):117-120.
PUBMED | CROSSREF
16. Kozomara A, Birgaoanu M, Griffiths-Jones S. miRBase: from microRNA sequences to function. Nucleic Acids Res. 2019;47(D1):D155-D162.
PUBMED | CROSSREF
17. Liu W, Wang X. Prediction of functional microRNA targets by integrative modeling of microRNA binding and target expression data. Genome Biol. 2019;20(1):18.
PUBMED | CROSSREF

18. Chen Y, Wang X. miRDB: an online database for prediction of functional microRNA targets. Nucleic Acids Res. 2020;48(D1):D127-D131.
PUBMED | CROSSREF

19. Sherman BT, Hao M, Qiu J, Jiao X, Baseler MW, Lane HC, et al. DAVID: a web server for functional enrichment analysis and functional annotation of gene lists (2021 update). Nucleic Acids Res. 2022;50(W1):W216-W221.
PUBMED | CROSSREF

20. RStudio Team. RStudio: integrated development for R [Internet]. Boston: RStudio Team; http://www.rstudio.com. Updated 2020. Accessed 2023 Jan 12.

21. Shannon P, Markiel A, Ozier O, Baliga NS, Wang JT, Ramage D, et al. Cytoscape: a software environment for integrated models of biomolecular interaction networks. Genome Res. 2003;13(11):2498-2504.
PUBMED | CROSSREF

22. Schmittgen TD, Livak KJ. Analyzing real-time PCR data by the comparative C(T) method. Nat Protoc. 2008;3(6):1101-1108.
PUBMED | CROSSREF

23. Hunt HD, Jadhao S, Swayne DE. Major histocompatibility complex and background genes in chickens influence susceptibility to high pathogenicity avian influenza virus. Avian Dis. 2010;54(1 Suppl):572-575.
PUBMED | CROSSREF

24. Haller O, Staeheli P, Kochs G. Protective role of interferon-induced Mx GTPases against influenza viruses. Rev Sci Tech. 2009;28(1):219-231.
PUBMED | CROSSREF

25. Jia YQ, Wang XL, Wang XW, Yan CQ, Lv CJ, Li XQ, et al. Common microRNA˜mRNA interactions in different newcastle disease virus-infected chicken embryonic visceral tissues. Int J Mol Sci. 2018;19(5):1291.
PUBMED | CROSSREF

26. Carlson CM, Turpin EA, Moser LA, O'Brien KB, Cline TD, Jones JC, et al. Transforming growth factor-β: activation by neuraminidase and role in highly pathogenic H5N1 influenza pathogenesis. PLoS Pathog. 2010;6(10):e1001136.
PUBMED | CROSSREF

27. Yu J, Sun X, Goie JY, Zhang Y. Regulation of host immune responses against influenza A virus infection by mitogen-activated protein kinases (MAPKs). Microorganisms. 2020;8(7):1067.
PUBMED | CROSSREF

28. Barjesteh N, Shojadoost B, Brisbin JT, Emam M, Hodgins DC, Nagy É, et al. Reduction of avian influenza virus shedding by administration of Toll-like receptor ligands to chickens. Vaccine. 2015;33(38):4843-4849.
PUBMED | CROSSREF

29. Wei Q, Xue H, Sun C, Li J, He H, Amevor FK, et al. Gga-miR-146b-3p promotes apoptosis and attenuate autophagy by targeting AKT1 in chicken granulosa cells. Theriogenology. 2022;190:52-64.
PUBMED | CROSSREF

30. Ehrhardt C, Wolff T, Pleschka S, Planz O, Beermann W, Bode JG, et al. Influenza A virus NS1 protein activates the PI3K/Akt pathway to mediate antiapoptotic signaling responses. J Virol. 2007;81(7):3058-3067.
PUBMED | CROSSREF

31. Duan X, Zhao M, Li X, Gao L, Cao H, Wang Y, et al. gga-miR-27b-3p enhances type I interferon expression and suppresses infectious bursal disease virus replication via targeting cellular suppressors of cytokine signaling 3 and 6 (SOCS3 and 6). Virus Res. 2020;281:197910.
PUBMED | CROSSREF

32. Zhao Y, Zhang K, Zou M, Sun Y, Peng X. gga-miR-451 negatively regulates *Mycoplasma gallisepticum* (HS strain)-induced inflammatory cytokine production via targeting YWHAZ. Int J Mol Sci. 2018;19(4):1191.
PUBMED | CROSSREF

33. Pham TT, Ban J, Hong Y, Lee J, Vu TH, Truong AD, et al. MicroRNA gga-miR-200a-3p modulates immune response via MAPK signaling pathway in chicken afflicted with necrotic enteritis. Vet Res. 2020;51(1):8.
PUBMED | CROSSREF

34. Lin HJ, Lin CW, Mersmann HJ, Ding ST. Sterol-O acyltransferase 1 is inhibited by gga-miR-181a-5p and gga-miR-429-3p through the TGFβ pathway in endodermal epithelial cells of Japanese quail. Comp Biochem Physiol B Biochem Mol Biol. 2020;240:110376.
PUBMED | CROSSREF

35. Chen F, Chen L, Li Y, Sang H, Zhang C, Yuan S, et al. traf3 positively regulates host innate immune resistance to influenza A virus infection. Front Cell Infect Microbiol. 2022;12:839625.
PUBMED | CROSSREF

36. Fric J, Zelante T, Wong AY, Mertes A, Yu HB, Ricciardi-Castagnoli P. NFAT control of innate immunity. Blood. 2012;120(7):1380-1389.
PUBMED | CROSSREF

37. Diehl N, Schaal H. Make yourself at home: viral hijacking of the PI3K/Akt signaling pathway. Viruses. 2013;5(12):3192-3212.
PUBMED | CROSSREF

38. Zhang C, Ni C, Lu H. Polo-like kinase 2: from principle to practice. Front Oncol. 2022;12:956225.
PUBMED | CROSSREF

39. Gotoh I, Adachi M, Nishida E. Identification and characterization of a novel MAP kinase kinase kinase, MLTK. J Biol Chem. 2001;276(6):4276-4286.
PUBMED | CROSSREF

40. Khiem D, Cyster JG, Schwarz JJ, Black BL. A p38 MAPK-MEF2C pathway regulates B-cell proliferation. Proc Natl Acad Sci U S A. 2008;105(44):17067-17072.
PUBMED | CROSSREF